see commentary on page 407

Fat redistribution and adipocyte transformation in uninephrectomized rats

Hai-Lu Zhao[1,5], Yi Sui[1,5], Jing Guan[1], Lan He[1], Xun Zhu[1], Rong-Rong Fan[1], Gang Xu[1], Alice P.S. Kong[1], Chung Shun Ho[2], Fernand M.M. Lai[3], Dewi K. Rowlands[4], Juliana C.N. Chan[1] and Peter C.Y. Tong[1]

[1]Department of Medicine and Therapeutics, The Chinese University of Hong Kong, Hong Kong SAR, China; [2]Department of Chemical Pathology, The Chinese University of Hong Kong, Hong Kong SAR, China; [3]Department of Anatomical and Cellular Pathology, The Chinese University of Hong Kong, Hong Kong SAR, China and [4]Laboratory Animal Services Centre, The Chinese University of Hong Kong, Hong Kong SAR, China

Dyslipidemia complicates renal function leading to disturbances of major homeostatic organs in the body. Here we examined the effect of chronic renal dysfunction induced by uninephrectomy on fat redistribution and lipid peroxidation in rats treated with an angiotensin-converting enzyme (ACE) inhibitor (lisinopril) for up to 10 months. Uninephrectomized rats developed fat redistribution and hypercholesterolemia typical of chronic renal failure when compared with sham-operated rats or lisinopril-treated uninephrectomized rats. The weight of the peri-renal fat was significantly less in the untreated compared to the lisinopril-treated uninephrectomized rats or those rats with a sham operation. We also found that there was a shift of heat-protecting unilocular adipocytes to heat-producing multilocular fat cells in the untreated uninephrectomized rats. Similarly in these rats we found a shift of subcutaneous and visceral fat to ectopic fat with excessive lipid accumulation and lipofuscin pigmentation. Lisinopril treatment prevented fat redistribution or transformation and lipid peroxidation. This study shows that ACE inhibition may prevent the fat anomalies associated with chronic renal dysfunction.

Kidney International (2008) **74,** 467–477; doi:10.1038/ki.2008.195; published online 21 May 2008

KEYWORDS: adipose; chronic renal failure; lipid; lipofuscin; unilateral nephrectomy

Correspondence: *Hai-Lu Zhao, Department of Medicine and Therapeutics, Prince of Wales Hospital, The Chinese University of Hong Kong, Shatin, NT, Hong Kong SAR, China. E-mail: zhaohailu@yahoo.com*

[5]These authors contributed equally to this work.

Received 28 November 2007; revised 27 January 2008; accepted 19 February 2008; published online 21 May 2008

The kidney is one of the major organs involved in whole-body homeostasis with its major functions being excretion of waste metabolites, regulation of blood pressure and lipid metabolism, secretion and degradation of hormones, production and utilization of systemic glucose.[1–3] It is well understood that chronic renal impairment is further complicated with high blood pressure,[4] deranged carbohydrate metabolism,[5] dyslipidemia,[6] and altered abdominal fat distribution,[7] but it is unclear whether the kidney is essential in normal fat function and adipose distribution.

Normally, each whole kidney is surrounded by layers of peri-renal fat mainly comprising large unilocular adipocytes (white adipose tissue), whereas the multilocular fat (brown adipose tissue) occupies the renal sinus.[8] The multilocular fat is specialized in heat production (thermogenesis), whereas the unilocular fat serves as heat protection and body cushioning,[9–11] Compared with the unilocular fat, the multilocular adipose tissue normally contains a higher proportion of fatty acids and phospholipids and a lower fraction of triglyceride in the form of neural fat.[12] Moreover, the presence of redox systems in microsomes of multilocular adipose tissue results in high activity of lipid peroxidation,[13] and lipid peroxidation of subcellular organelles gives lipofuscin pigments.[14,15] Therefore, lipofuscin pigments are morphological markers reflecting cellular activity of lipid peroxidation.

Continuous transformation between the multilocular adipocyte and the unilocular fat cell occurs throughout life.[11,16] In prolonged malnutrition[17] or in the emaciation associated with chronic illness,[11] unilocular adipose tissue gives up most of its stored lipid and reverts to the highly thermogenic tissue made up of multilocular cells. In chronic kidney disease, there is an increased adiponectin production in association with metabolic abnormalities,[18] whereas in non-diabetic patients with hemodialysis, altered abdominal fat distribution is associated with altered serum lipid profile.[7] In this study, we hypothesize that the kidney is essential in normal fat function and adipose distribution and that chronic renal dysfunction, induced by uninephrectomy, leads to altered adipose distribution and lipid peroxidation in

association with hypercholesterolemia. Normalization of renal function by treatment should therefore prevent adipose dysfunction and ectopic fat accumulation, thus potentially reduce cardiovascular disease and cerebrovascular disease risks, which are leading causes of death in patients with renal disease.

RESULTS

Renal impairment induced by uninephrectomy

First, we assessed the uninephrectomy-induced renal impairment with histological examination at 4, 7, and 10 months post-operation. Compared with sham rats (Figure 1, dashed line), the untreated uninephrectomized (UNX) rats (Figure 1, solid line) had significantly higher serum creatinine (Figure 1a) and urea (Figure 1b), higher urine total protein/creatinine (Figure 1c), and lower serum albumin (Figure 1d). The untreated UNX rats developed uremia at 10 months post-operation (13 months of age). Treatment with lisinopril prevented the development of chronic renal failure (Figure 1, light line).

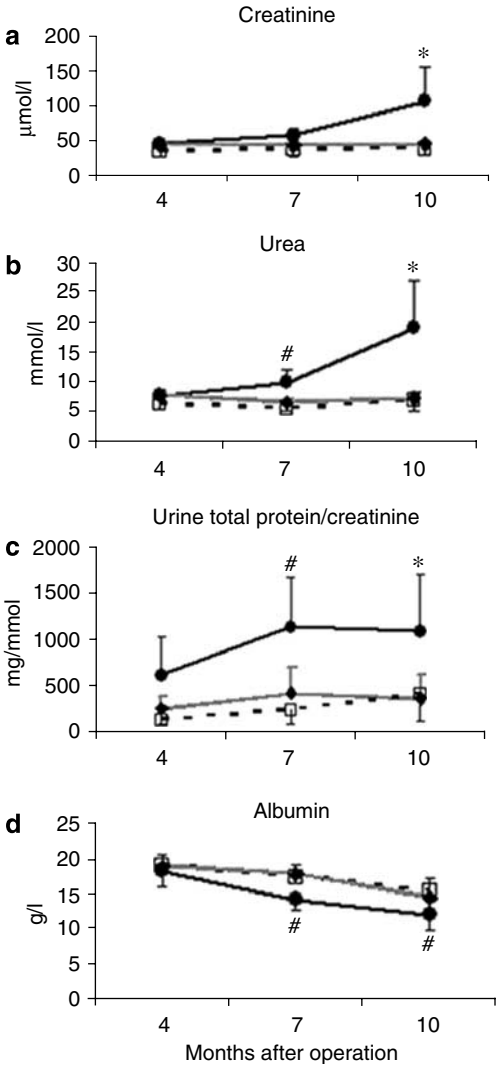

Figure 1 | Chronic renal failure after uninephrectomy. Serum creatinine (**a**), urea (**b**), and albumin (**d**), and urine total protein/creatinine (**c**) were measured in sham rats (square, dashed), uninephrectomized rats (UNX, circle, dark solid), and UNX rats treated with the ACEI lisinopril (ACEI, diamond, light solid) at 4, 7, and 10 months after operation. The untreated UNX rats developed chronic renal failure, whereas ACEI treatment prevented the development of chronic renal failure. Data are mean ± s.d., $^{\#}P<0.05$, $^{*}P<0.01$.

The weight of the remnant kidney (4.5 ± 1.2 g) and the ratio of the remnant kidney weight to total body weight (0.87 ± 0.23%) in UNX rats were more than twofold greater of those of the corresponding right kidney in sham rats (weight 2.1 ± 0.2 g; ratio 0.35 ± 0.06%; all $P<0.001$) at 10 months post-operation, whereas treatment with lisinopril significantly reduced the remnant kidney hypertrophy (weight 3.64 ± 0.4 g; ratio 0.58 ± 0.06%; all $P<0.001$). The increase in weight of the remnant kidney strongly correlated with increased blood urea ($r=0.8812$, $P<0.001$) and creatinine ($r=0.781$, $P<0.001$). Histopathological examination revealed normal kidney structures in sham rats (Figure 2a–c) but progressive glomerulosclerosis, tubular atrophy, arteriolar hyalinosis, fibrosis, and chronic inflammatory infiltrates in the remnant kidneys (Figure 2d–f). The untreated UNX rats showed end-stage renal disease at 10 months post-operation, whereas treatment with lisinopril largely attenuated these renal structural damages (Figure 2g–i).

Hypercholesterolemia associated with chronic renal dysfunction

We then examined the uninephrectomy-induced hypercholesterolemia at 4, 7, and 10 months post-operation and the association of dyslipidemia with chronic renal dysfunction (Figure 3). Compared with sham rats, UNX rats had significantly higher serum total cholesterol (Figure 3a), triglycerides (Figure 3b), low-density lipoprotein (LDL) cholesterol (Figure 3c), and high-density lipoprotein (HDL) cholesterol (Figure 3d). The untreated UNX rats developed hypercholesterolemia at 10 months post-operation (13 months of age), whereas treatment with lisinopril substantially prevented the development of persistent hypercholesterolemia (Figure 3).

An analysis using Pearson's correlation coefficient indicated strong associations between serum creatinine and total cholesterol ($r=0.660$, $P<0.001$), triglyceride ($r=0.563$, $P<0.001$), LDL ($r=0.881$, $P<0.001$) and HDL cholesterol ($r=0.638$, $P<0.001$), and between serum urea and total cholesterol ($r=0.724$, $P<0.001$), triglyceride ($r=0.640$, $P<0.001$), LDL ($r=0.558$, $P<0.001$) and HDL cholesterol ($r=0.670$, $P<0.001$). These data indicate a close relationship between renal function and blood lipids.

Body weight and daily food consumption were similar among the three groups of rats (Figure 4a and b). Daily water intake (Figure 4c) and urine volume (Figure 4d) at 7 and 10 months after operation were significantly higher in UNX rats than in sham rats and in UNX rats treated with lisinopril (all $P<0.05$).

Adipose distribution and lipofuscin accumulation

We performed histological examination of fat deposits to investigate the uninephrectomy-induced adipose distribution

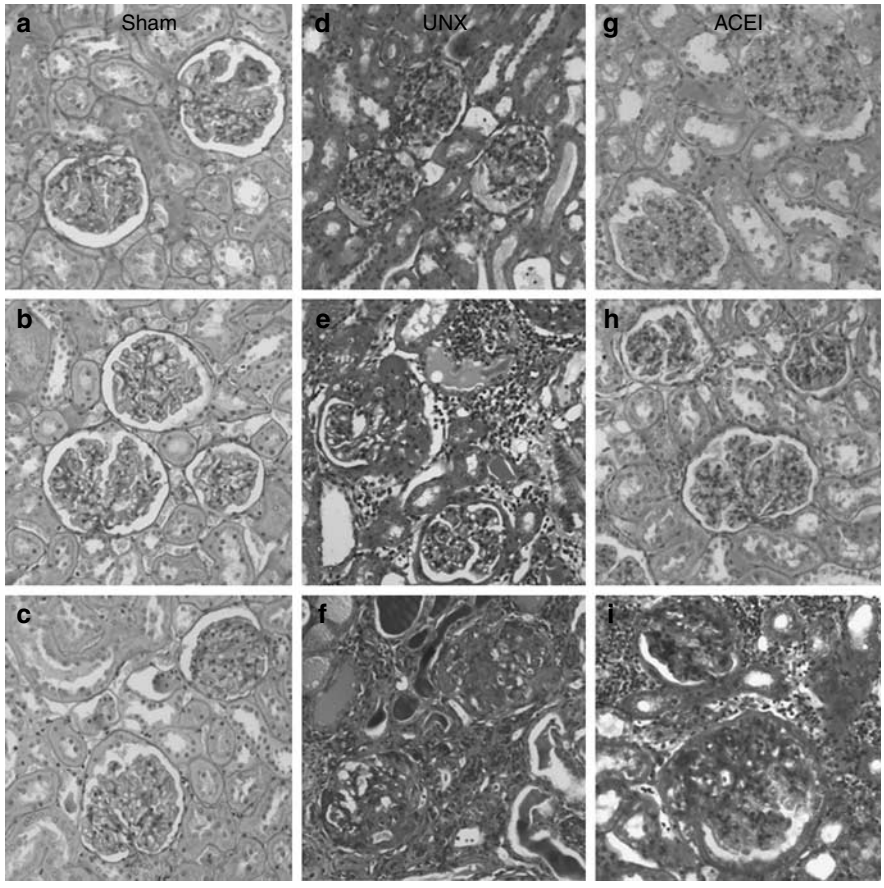

Figure 2 | Renal structural damages after uninephrectomy. Periodic acid Schiff (PAS) stain was performed on kidney tissue sections of sham rats (**a**–**c**), untreated uninephrectomized rats (UNX, **d**–**f**), and the ACEI lisinopril-treated UNX rats (ACEI, **g**–**i**) at 4 (**a**, **d**, **g**), 7 (**b**, **e**, **h**), and 10 (**c**, **f**, **i**) months after operation. The UNX rats (**d**–**f**) demonstrated severe glomerulosclerosis, chronic interstitial inflammatory infiltration, tubular atrophy, and casts. These renal lesions were largely attenuated with the ACEI treatment (**g**–**i**). Original magnification, $\times 100$.

(Figures 5–7) and lipofuscin accumulation (Figure 8). By 4, 7, and 10 months post-operation, fat deposits in the peri-renal capsule, omentum, mesenteries, and abdominal walls were significantly diminished in the UNX rats than in sham rats, whereas treatment with lisinopril mainly prevented the adipose loss in these areas. The weight of the peri-renal fat was 2.1 ± 1.0 g in the untreated UNX rats, 3.2 ± 0.3 g in the angiotensin-converting enzyme (ACEI)-treated UNX rats, and 3.2 ± 0.2 g in sham rats (analysis of variance $P = 0.028$). Light microscopy demonstrated that the peri-renal adipose tissues mainly contained large unilocular cells in sham rats (Figure 5a–c), polygonal multilocular cells in UNX rats (Figure 5d–f), and mixed unilocular and multilocular cells in the treated UNX rats (Figure 5g–i). These findings suggest that the loss of the large unilocular adipocytes and the transformation of the large unilocular adipocytes into the multilocular cells may be associated with the diminished peri-renal adipose mass induced by uninephrectomy.

Increased ectopic fat deposits were found in the remnant kidneys (Figure 6) and other solid organs (Figure 7), while in sham rats, fat deposits were confined within the renal sinus (Figure 6a, inset). Neither the renal cortex nor the renal medulla in sham kidneys contained adipose tissue (Figure 6a–c), but in contrast, UNX rats showed fat infiltration in the inner cortex (Figure 6d–f, insets). The fat infiltration was also frequently surrounded by patches of chronic inflammatory infiltrates. By 10 months post-uninephrectomy, infiltrated adipose tissues comprising of small adipocytes were found in 3–9 of 20 fields randomly examined at magnification $\times 200$, but treatment with lisinopril generally attenuated the fat infiltration in the remnant kidney (Figure 6g–i). These results provide evidence that renal cortex contains adipose tissue in rats with uninephrectomy-induced chronic renal insufficiency.

Uninephrectomy-induced ectopic fat deposits were also often found in other solid organs (Figure 7). In sham rats, lipid accumulation in hepatocytes (Figure 7a), pancreatic islets (Figure 7b), and in adrenal glands (Figure 7c) were rarely identified, but the untreated UNX rats frequently showed hepatosteatosis (Figure 7d), pancreatic lipomatosis (Figure 7e), and fatty changes in the zona fasciculate of the adrenal glands (Figure 7f). However, little ectopic lipid accumulation was observed in the UNX rats treated with lisinopril (Figure 7g–i), suggesting an association of ectopic fat accumulation with chronic renal failure in rats with uninephrectomy.

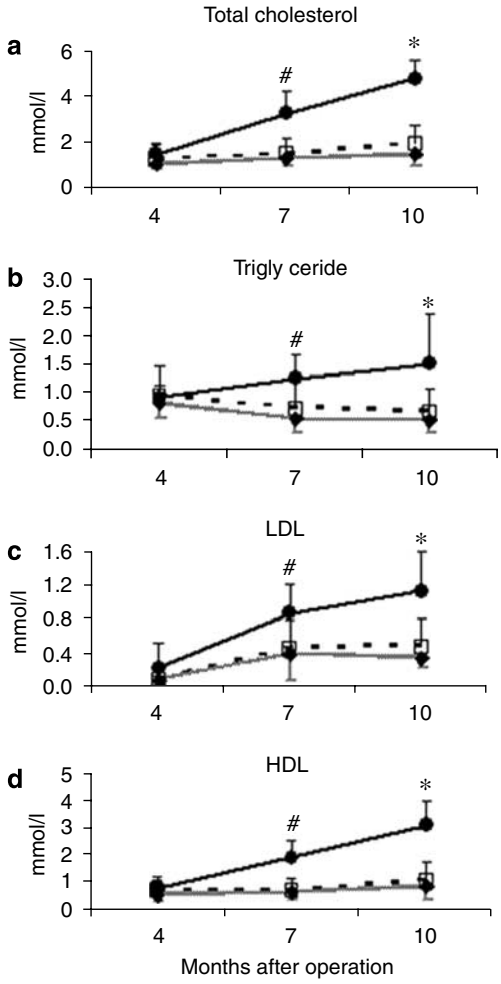

Figure 3 | Hypercholesterolemia after uninephrectomy. Serum total cholesterol (**a**), triglyceride (**b**), LDL cholesterol (**c**), and HDL cholesterol (**d**) were measured in sham rats (square, dashed), uninephrectomized rats (UNX, circle, dark solid), and the ACEI lisinopril-treated UNX rats (ACEI, diamond, light solid) at 4, 7, and 10 months after operation. The UNX rats developed hypercholesterolemia, and the lipid abnormalities were prevented by the ACEI treatment associated with normalized renal functions. Data are mean ± s.d., $^{\#}P<0.05$, $^{*}P<0.01$.

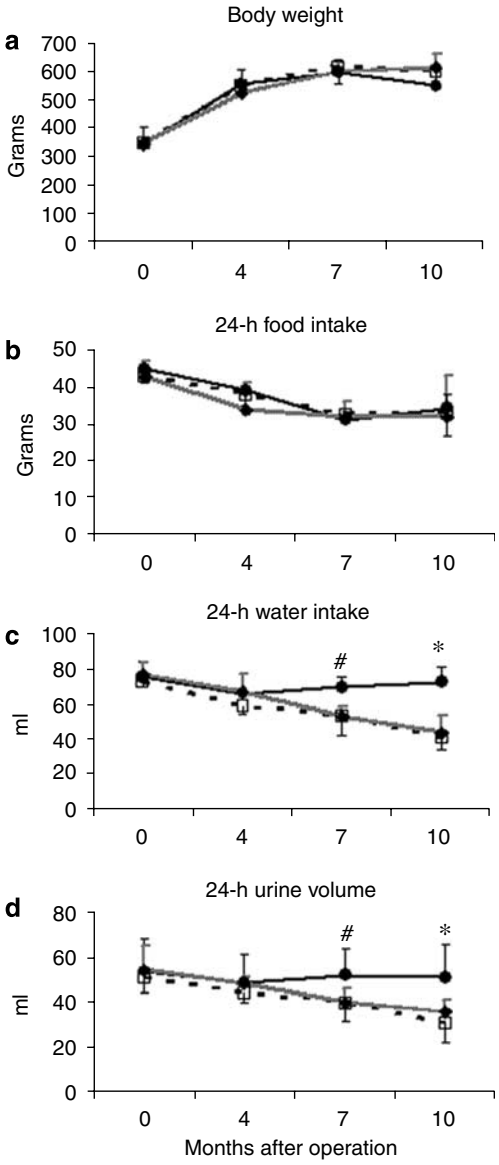

Figure 4 | Metabolic characteristics after uninephrectomy. Body weight (**a**) and average 24-h intake of food (**b**) and water (**c**) and urine volume (**d**) in sham rats (square, dashed), uninephrectomized rats (UNX, circle, dark solid), and the ACEI lisinopril-treated UNX rats (ACEI, diamond, light solid) were monitored at 0, 4, 7, and 10 months after operation. The body weight and food intake were similar among the three groups, whereas daily water intake and urine volume were higher in UNX rats than in sham rats and in the ACEI-treated UNX rats. Data are mean ± s.d., $^{\#}P<0.05$, $^{*}P<0.01$.

Lipofuscin, characterized by fine brown pigment granules, was identified to reflect the peroxidation of unsaturated fatty acids (Figure 8). In sham rats, cells with lipofuscin were rarely found, but at 4, 7, and 10 months post-uninephrectomy, UNX rats showed frequent lipofuscin-laden cells accompanied by chronic inflammation and fibrosis in the kidney (Figure 8a), liver (Figure 8b), and pancreas (Figure 8c). Treatment with lisinopril prevented the generalized accumulation of the lipofuscin-containing cells, again providing morphological evidence for increased lipid peroxidation associated with uninephrectomy-induced chronic renal dysfunction.

Elevation of fasting blood glucose and insulin concentrations

Fasting plasma glucose (Figure 9a) and serum insulin (Figure 9b) were measured, and homeostasis model assessment-estimated insulin resistance (HOMA-IR) (Figure 9c) was calculated to assess metabolic risk factors (Figure 9). Compared with sham- and ACEI-treated UNX rats, untreated UNX rats showed elevated fasting plasma glucose levels at 7 and 10 months after uninephrectomy. At 4 months post-operation, fasting serum insulin levels in UNX rats were elevated. Surprisingly, HOMA-IR was not significantly different among the three groups of animals. The consequence of adipose redistribution and adipocyte transformation in chronic renal dysfunction warrants future studies.

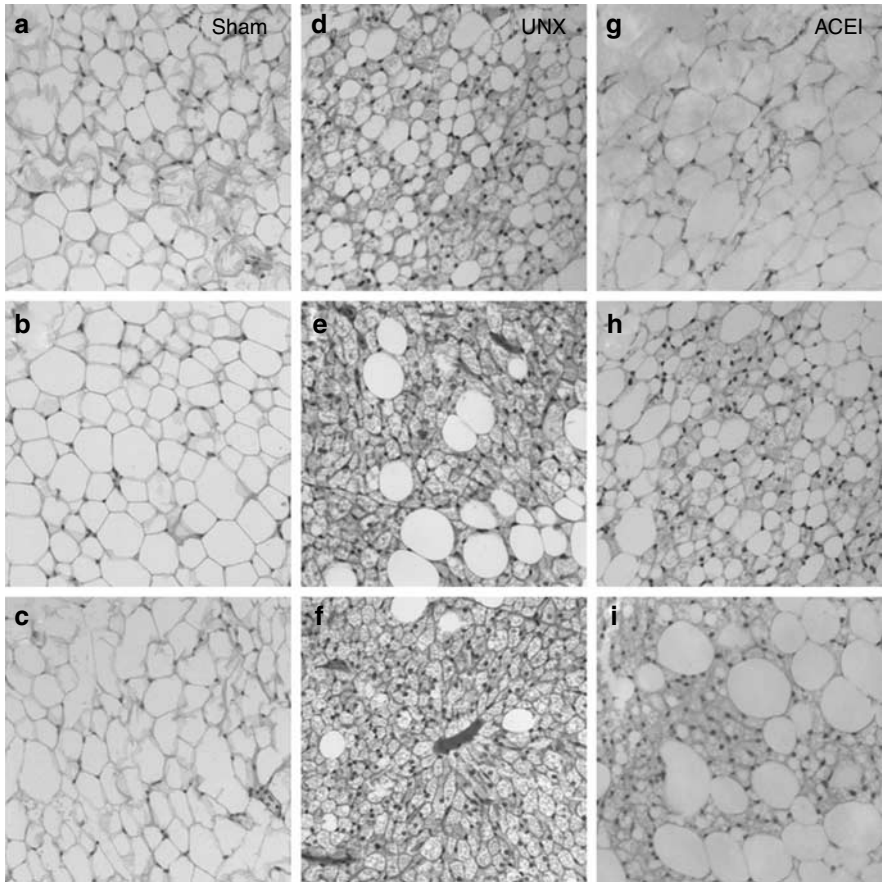

Figure 5 | Multilocular adipocytes of the peri-renal adipose tissues after uninephrectomy. Periodic acid Schiff (PAS) stain was performed on peri-renal adipose tissue sections of sham rats (**a**–**c**), untreated uninephrectomized rats (UNX, **d**–**f**), and the ACEI lisinopril-treated UNX rats (ACEI, **g**–**i**) at 4 (**a**, **d**, **g**), 7 (**b**, **e**, **h**), and 10 (**c**, **f**, **i**) months after operation. The UNX rats demonstrated remarkable transformation of the heat-protecting unilocular adipocytes into the heat-generating multilocular cells. The adipose transformation was largely attenuated with the ACEI treatment (**g**–**i**). Original magnification, $\times 100$.

Expression of local HMG-CoA reductase

HMG-CoA reductase (HMGCR) is the rate-controlling enzyme for cholesterol synthesis. Western blotting of local HMGCR was thus performed to explore potential links between the abnormal fat deposition and hyperlipidemia after uninephrectomy (Figure 10). Interestingly, HMGCR expression of the liver (Figure 10b) was similar among the three groups of animals. In contrast, renal HMGCR expression (Figure 10a) was increased in the untreated UNX rats but not in sham or ACEI animals. These results strongly support the notion that the kidney is an essential organ in maintaining lipid homeostasis, and chronic renal insufficiency may enhance renal HMGCR expression associated with hyperlipidemia and fat dysfunction (adiposopathy).

Chronic inflammatory infiltration and fibrosis

Double immunofluorescent microscopy showed inflammatory infiltration and fibrosis in association with uninephrectomy-induced abnormal fat deposition (Figure 11). Peri-renal fat of the untreated UNX rats (Figure 11b) mainly composed of multilocular cells reactive for the proinflammatory, profibrotic cytokine transforming growth factor-β (TGF-β), whereas the unilocular adipocytes of peri-renal fat in sham rats were negative for TGF-β (Figure 11a). Increased TGF-β immunoreactivity was also found in the renal adipocytes (Figure 11c), which were negative for Glut4 glucose transporters or a macrophage-specific marker CD68 (Figure 11d). CD68-stained macrophages were frequently present at the peripheral region of renal adipocytes. Renal adipocytes were usually intermixed with α-smooth muscle actin-labeled cells (Figure 11c), an activated cell type capable of producing extracellular matrix. Increased TGF-β expression was also shown in lipofuscin-laden cells of the liver (Figure 11e). These results suggest potential associations between ectopic fat deposition, lipid peroxidation, chronic inflammation and fibrosis.

DISCUSSION

This study demonstrates the adipose redistribution, adipocyte transformation, and cellular lipid peroxidation in male adult UNX Sprague–Dawley rats and provides evidence that treatment with an ACEI, such as lisinopril, can prevent the development of chronic renal impairments associated with

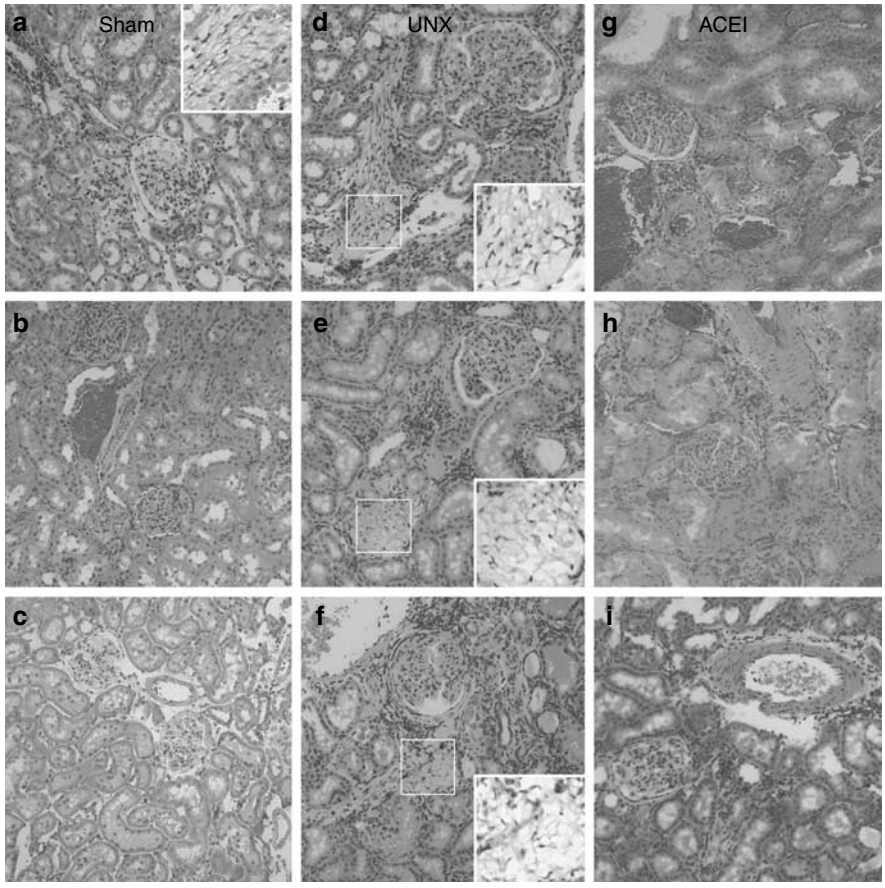

Figure 6 | Adipose deposits in the remnant kidney. Hematoxylin-eosin (HE) stain was performed on kidney tissue sections of sham rats (**a**–**c**), uninephrectomized rats (UNX, **d**–**f**), and the ACEI lisinopril-treated UNX rats (ACEI, **g**–**i**) at 4 (**a**, **d**, **g**), 7 (**b**, **e**, **h**), and 10 (**c**, **f**, **i**) months after operation. Sham rats (**a**–**c**) showed adipose distribution in the renal sinus (**a**, inset), but not the renal cortex. In contrast, UNX rats (**d**–**f**) demonstrated remarkable fat infiltration (**d**–**f**, insets) in renal cortex in association with glomerulosclerosis. The fat infiltration was largely attenuated with the ACEI treatment (**g**–**i**). Original magnification, $\times 100$.

hypercholesterolemia in the rats with uninephrectomy. Adipose distribution and adipocyte transformation in UNX rats might possibly be related to the following molecular, metabolic, and cellular abnormalities: (1) increased expression of renal HMGCR, (2) hyperlipidemia characterized by high total cholesterol, LDL cholesterol, HDL cholesterol, and triglyceride, (3) elevated fasting blood glucose and insulin, (4) chronic inflammatory infiltration and fibrosis, and (5) increased cellular lipid peroxidation.

The initial cause of the adipose distribution and adipocyte transformation appears to be due to uninephrectomy-induced chronic renal dysfunction. The nephrectomized rat model has long been used as an animal model to study nephropathy. However, most studies involved models set up by 5/6 or 7/8 nephrectomy,[19,20] hence the renal failure was relatively acute and severe and observation periods were shorter (<4 months). In our experiments, we selected a uninephrectomy rat model and went through a 10-month observation, which reflects a chronic model that is closer to the real reactions of fat redistribution and lipid dysmetabolism in human kidney donors and subjects with chronic renal dysfunction. Moreover, nephrectomy is a severe procedure that produces a myriad of effects on many systems including the renin–angiotensin–aldosterone systems and the endocrine organs,[21,22] demonstrating that the kidney is one of the most important homeostasis organs.

Our results demonstrated that compared with sham rats, the UNX rats had a lower proportion of body fat due to severe renal insufficiency. Rats with uninephrectomy developed chronic proteinuria in association with massive deposits of lipids, which were shown to consist mainly of free and esterified cholesterol,[23] as have prior studies in subtotally nephrectomized animals demonstrated a significant correlation between glomerular filtration rate and body fat content.[24] Consistent with the present study, the renal impairments and lipid deposition were generally prevented by ACEI treatments in Nagase analbuminemic rats, after 5/6 nephrectomy, which usually exhibit severe glomerulosclerosis, persistent hypercholesterolemia, and massive lipid deposition.[25] Additionally, clinical studies using computed tomography have previously demonstrated a significant decrease in body fat area and subcutaneous adipose tissue in parallel to an increase in visceral fat mass associated with disturbance of the serum lipid profile in non-diabetic

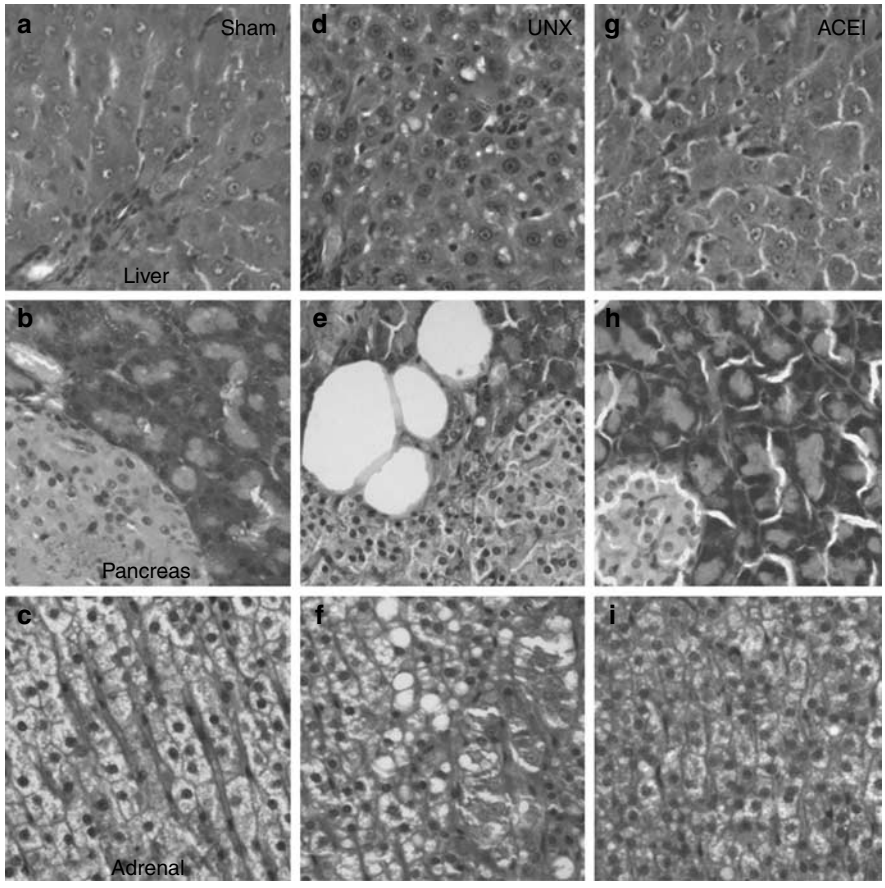

Figure 7 | Ectopic lipid accumulation after uninephrectomy. Periodic acid Schiff (PAS) stain was performed on tissue sections of livers (**a**, **d**, **g**), pancreata (**b**, **e**, **h**), and adrenal glands (**c**, **f**, **i**) from sham rats (**a**–**c**), untreated uninephrectomized rats (UNX, **d**–**f**), and the ACEI lisinopril-treated UNX rats (ACEI, **g**–**i**) at 10 months after operation. The UNX rats demonstrated ectopic fat deposits characterized by hepatic steatosis (**d**), pancreatic lipomatosis (**e**), and adrenal fatty change (**f**). The ectopic lipid accumulation was largely attenuated with the ACEI treatment (**g**–**i**). Original magnification, $\times 100$.

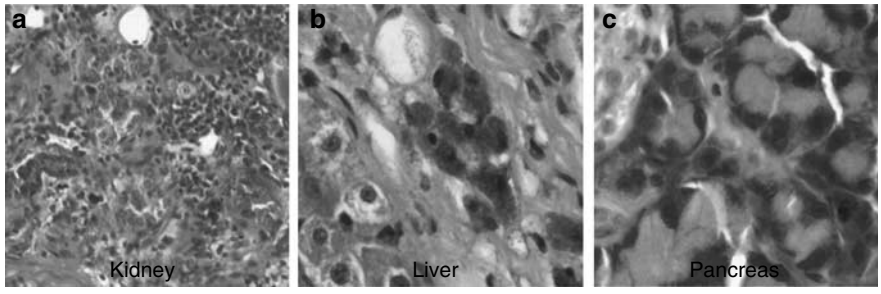

Figure 8 | Lipofuscin-laden cells after uninephrectomy. Representative micrographs of uninephrectomized rats 10 months after operation show abundant lipofuscin-laden cells in the kidney (**a**), liver (**b**), and pancreas (**c**). The lipofuscin pigments were pink cytoplasmic granules reactive for periodic acid Schiff. Original magnification, $\times 200$.

hemodialysis patients.[7] Abnormal fat partition and excessive ectopic fat deposition are also known to have potentially pathogenic adverse effects on metabolism, immune, hormone, and circulation responses, which may lead to disturbance of whole-body homeostasis.

We also reported shifts of the heat-producing multilocular fat cells from the heat-protecting unilocular adipocytes and of the ectopic fat from both the subcutaneous and visceral fats, suggesting a relationship between chronic renal dysfunction and persistent hypercholesterolemia. Accumulation of triglyceride-rich lipoproteins in renal insufficiency may be related to an increased expression of lipogenic enzyme[26] and fatty acid synthase,[27] a functional impairment in lipoprotein lipase,[28] a decrease in the total concentration of glucose transporters,[29] as well as downregulation of leptin mRNA,[30] lipoprotein lipase,[31,32] and very LDL receptor.[33] In

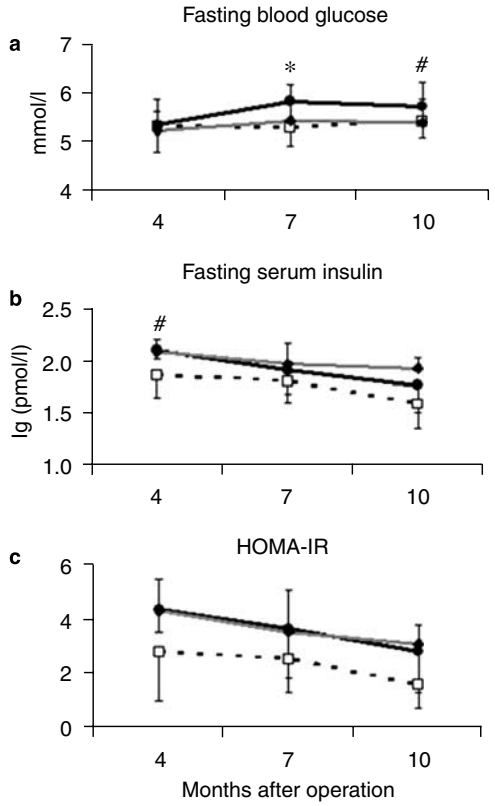

Figure 9 | Blood glucose and insulin levels after uninephrectomy. Fasting (**a**) plasma glucose, (**b**) serum insulin, and (**c**) homeostasis model assessment-estimated insulin resistance (HOMA-IR) were measured in sham rats (square, dashed), uninephrectomized rats (UNX, circle, dark solid), and the ACEI lisinopril-treated UNX rats (ACEI, diamond, light solid) at 4, 7, and 10 months after operation. The UNX rats developed hyperglycemia, and the glycemic abnormalities were prevented by the ACEI treatment associated with normalized renal functions. Data are mean ± s.d., $^{\#}P<0.05$, $^{*}P<0.01$.

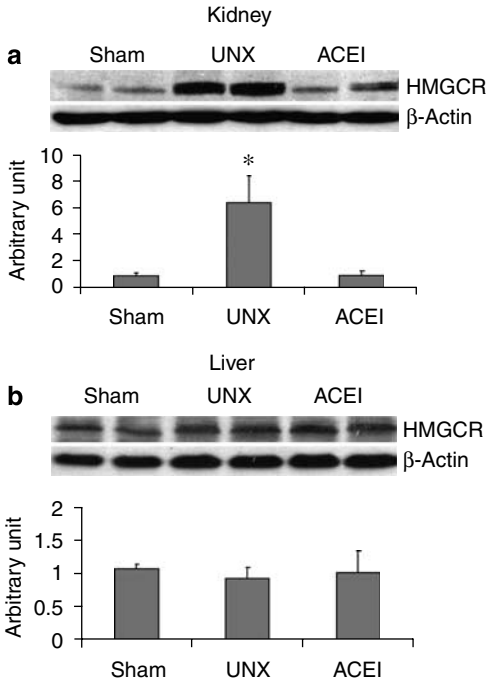

Figure 10 | Western blot of local HMG-CoA reductase (HMGCR). Equal amounts of tissue lysates (100 μg) were subjected to SDS-PAGE to immunoblot for HMGCR. HMGCR protein of the kidney (**a**) and liver (**b**) at 10 months post-operation was quantified by densitometric scanning and image analysis software. Pixel intensity was normalized and a value of 1 was assigned to the protein amount of sham rats. Data are mean ± s.d., $^{*}P<0.01$.

uremic animals, adipose tissue triglyceride content but not the HMGCR activity of liver microsomes was decreased.[34] In this study, HMGCR expression of the liver was consistently unchanged. Instead, HMGCR expression of the kidney was increased in the untreated UNX rats, suggesting that renal HMGCR might contribute to the uninephrectomy-induced adiposopathy. Adiposopathy is also reflected by increased secretion of functional adipokines (for example, adiponectin, leptin) and inflammatory cytokines (for example, tumor necrosis factor-α, interleukin-6).[35,36] Plasma adipokine levels are related to several metabolic risk factors in patients with chronic kidney disease[36] or end-stage renal disease.[37] In the present study, plasma glucose levels and serum insulin concentrations but not HOMA-IR was elevated in the untreated UNX rats. All these data implicate that the kidney is essential to the whole-body metabolic homeostasis, and chronic renal insufficiency may cause adiposopathy characterized by hyperlipidemia, adipose redistribution, and adipocyte transformation.

Our study also showed significant ectopic fat deposition and lipid peroxidation, with the accumulated fat consisting of lipid-depleted multilocular cells, which are believed to be produced after oxidation of fat for heat production (thermogenesis).[38] Interestingly, lipid deposition in the glomeruli occurred secondary to hyperlipidemia in rats following subtotal nephrectomy, indicating an association between hyperlipidemia and ectopic fat accumulation.[39,40] Glomerular lipid deposition has been implicated in the development of glomerulosclerosis in rats after renal ablation.[41] Indeed, experimental glomerulosclerosis is associated with hyperlipidemia and the deposition of lipid in glomeruli, and cholesterol feeding following uninephrectomy in the rats leads to glomerular hypertrophy.[40] In agreement with our studies, treatments with an ACEI enalapril,[25] β-blocking drug carvedilol,[20] or dietary vitamin E (α-tocopherol)[42,43] have been shown to prevent renal impairments and lipid deposition in subtotally nephrectomized rats. Other drugs that could preserve the renal function in rats with 5/6 nephrectomy include the specific cholesterol synthesis inhibitor mevinolin[44] or the HMGCR inhibitor lovastatin.[45] Taken together, these findings indicate that the kidney is central to the normal fat function, adipose distribution, and lipid metabolism.

The high prevalence of chronic renal failure and high number of living kidney donors, for renal transplantation,

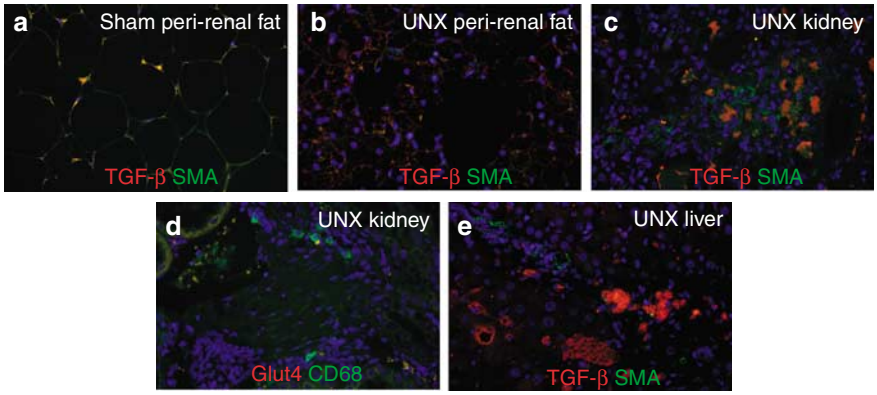

Figure 11 | Immunofluorescent microscopy of chronic inflammation and fibrosis. Tissue sections were obtained from the peri-renal fat (**a**, **b**), remnant kidney (**c**, **d**) and liver (**e**) at 10 months after operation and double stained for (**a**–**c**, **e**) transforming growth factor-β (TGF-β, red) and α-smooth muscle actin (SMA, green) as well as for (**d**) Glut4 glucose transporters (red) and macrophage-specific marker CD68 (green). Uninephrectomy led to increased expression of TGF-β in multilocular fat cells (**b**), renal adipocytes (**c**), and hepatic lipofuscin-laden cells that were frequently intermixed with SMA-positive cells. Renal adipocytes were negative for Glut4 or CD68, whereas CD68-reactive macrophages were usually found at the peripheral region of renal adipose deposition. Original magnification, $\times 200$.

prompted this study of fat redistribution and lipid metabolism. In all, the findings of this study indicate an important role of the kidney in maintaining normal fat distribution and lipid homeostasis independently and through coordination with other organs, particularly the adrenal gland, the liver, and the pancreas. Chronic kidney disease is a common public health problem which affects approximately 12% of adults in the United States.[46] Clinical assessment of long-term risks of whole-body disturbance in kidney donors and in patients with chronic renal disease is therefore strongly recommended so as to reduce cardiovascular risk in these patients.

MATERIALS AND METHODS

Animals

Three-month-old male Sprague–Dawley rats weighing initially between 300 and 350 g were obtained from the Laboratory Animal Services Centre at the Chinese University of Hong Kong. The animals were caged in pairs, housed at $23 \pm 1^{\circ}C$ with a 12-h dark–light cycle, having free access to water, and fed on a standard laboratory rat diet (5001 Rodent Diet; LabDiet, St Louis, MO, USA). The total duration of the studies was 10 months.

Ethical approval for animal studies was according to the Animal Experimentation Ethics Committee of The Chinese University of Hong Kong, and in accordance with the Animals (Control of Experiments) Ordinance of the Department of Health of the Hong Kong SAR Government.

Unilateral nephrectomy

Rats were anesthetized with a ketamine (75 mg/kg; Alfasan, Woerden, Holland) and xalyzine (10 mg/kg; Alfasan) and subjected to a sham operation ($n = 16$), left nephrectomy (UNX, $n = 16$), or UNX treated with ACEI lisinopril (ACEI, $n = 16$). Lisinopril was dissolved in sterile distilled water, with once daily dosage of 4 mg per kg body weight. All the sham and UNX rats were also gavaged with distilled water (3 ml) as placebo control. The left kidney was exposed via a flank 1−1.5 cm length incision and was removed, leaving the adrenal gland intact. Sham-operated rats underwent anesthesia and ventral laparotomy without removal of the left kidney. At 4, 7, and 10 months post-operation, 3, 5, and 8 rats from each group were killed for biochemical and histopathological assessments.

Biochemical studies

Body weight and average 24-h intake of water and food were monitored monthly. At 4, 7, and 10 months post-operation, 24-h urine samples were collected using metabolic cages (Iluang Qiao Yin Xing Animal Cage & Equipments Factory, Suzhou, China). Fasting blood samples were taken for the measurement of glucose, insulin, total cholesterol, triglyceride, LDL cholesterol, HDL cholesterol, total protein, albumin, and renal functions. The rat serum measurements were performed on a UniCel DxC600 System (Beckman Coulter, Fullerton, CA, USA). Total cholesterol was measured by an enzymatic method and triglycerides were measured by an enzymatic method without glycerol blanking. HDL cholesterol was measured by an indirect method in which phosphotungstic acid reagent was used to precipitate the LDL and very LDL cholesterol and the remaining HDL cholesterol was measured by the total cholesterol method. The HDL-precipitating reagent was purchased from Thermo Electron (Noble Park, Victoria, Australia). LDL cholesterol concentration was calculated with the use of Friedewald's formula.[47] Fasting serum insulin concentrations were measured using enzyme immunoassay and rat insulin ELISA kit (Mercodia, Uppsala, Sweden). HOMA-IR was calculated with the formula HOMA-IR = fasting insulin (mU/l) × fasting blood glucose (mmol/l)/22.5.

Fasting serum urea (enzymatic method) and serum/urine creatinine (Jaffe kinetic method) were measured using a Modular Analytics analyzer (Roche Diagnostics GmbH, Mannheim, Germany), and reagent kits were supplied by the manufacturer. All reagents were used according to the manufacturer's instruction and the analytical performance of these methods was within the manufacturer's specifications.

Histopathological examination

Rats were killed at 4, 7, and 10 months post-operation. Gross examination of subcutaneous adipose tissues in abdominal wall and of visceral fats in peri-renal capsule, omentum, and mesenteries were performed to assess fat distribution. Kidneys, peri-renal

adipose tissue, adrenal glands, spleens, pancreata, and livers were removed, weighed, and processed for light microscopy. Specimens, including peri-renal adipose tissues, were fixed in 10% neutral formaldehyde and embedded in paraffin. Serial cross sections (4 μm) were cut perpendicular to the longest axis of the solid organs. Sections were stained with hematoxylin-eosin and periodic acid Schiff. Stained slides were examined with a Zeiss Axioplan 2 imaging microscope (Carl Zeiss, Hamburg, Germany), and slide reviewers were blinded to treatment group. Representative images were automatically captured using a digital spot camera.

Western blot

Tissue proteins from kidney and liver were isolated. Briefly, tissue was homogenized in a buffer containing 50 mmol/l Tris-HCl (pH 7.4), 150 mmol/l NaCl, 1 mmol/l phenylmethylsulfonyl fluoride, 1 mmol/l EDTA, 1% sodium deoxycholate, 1% Triton X-100, 1% sodium dodecyl sulfate, and 5% protein enzyme inhibitor cocktail (cat no. P2714; Sigma, St Louis, MO, USA). The homogenate was centrifuged at 13 000 *rpm* for 10 min at 4°C. The resulting supernatant was removed, and protein concentrations in the supernatant were determined by the BCA Protein Assay Kit (cat no. 23225; ThermoFisher Scientific, Waltham, MA, USA) using bovine serum albumin as the standard. Tissue lysates (100 μg) and prestained molecular weight markers (Bio-Rad, Hercules, CA, USA) were loaded onto SDS-polyacrylamide electrophoresis gels (PAGE) (4% acrylamide stacking gel and 8% running gel). The resolved proteins were then transferred onto nitrocellulose membranes. The membranes were blocked for 1 h at room temperature with 5% skimmed milk, incubated with a rabbit anti-rat polyclonal HMGCR antibody (cat no. 07-457; Upstate, Temecula, MA, USA) diluted 1:1000 in Tris-buffered saline containing 0.05% Tween 20 (Tris-buffered saline-T) with 5% skimmed milk overnight at 4°C. After washing with Tris-buffered saline-T, membranes were incubated with anti-rabbit secondary antibody conjugated to horseradish peroxidase (cat no. 12-348; Upstate) with a dilution of 1:2000. Proteins were detected by enhanced chemiluminescence (Amersham, Piscataway, NJ) on hyperfilm. A major protein band with approximately 90 kDa was detected for the HMGCR. To ensure equal loading of proteins, membranes were incubated and probed with a polyclonal anti-β-actin antibody (cat no. ab8227; Abcam, Cambridge, MA, USA) with a dilution of 1:10 000, which recognizes the β-actin protein at approximately 43 kDa. Signals were quantitated by densitometry and corrected for the β-actin signal, using the Kodak Digital Image station 440CF and the ID Image Analysis software program.

Immunofluorescent microscopy

Tissue sections (4 μm) from the peri-renal fat, kidney, and liver were double stained for (1) polyclonal TGF-β (cat no. SC-146, dilution 1:200; Santa Cruz Biotechnology, Santa Cruz, CA, USA) and monoclonal α-smooth muscle actin (cat no. N1584, dilution 1:10; Dako, Carpinteria, CA, USA) and (2) polyclonal Glut4 (cat no. SC-7938, dilution 1:100; Santa Cruz) and monoclonal CD68 (cat no. M0876, dilution 1:100; Dako). Tissue slides were blocked with 1% bovine serum albumin for 30 min before the treatment with the primary antibodies for 1 h at room temperature. Goat, rabbit, and mouse serum were used as negative controls to replace the primary antibodies. Immunofluorescence was detected with appropriate secondary antibodies (dilution 1:200) conjugated with Alexa 488 (green) or Alexa 568 (red), and cell nuclei were counterstained with DAPI (1:200; Invitrogen Corp., Carlsbad, CA, USA). Slides were mounted with an anti-fading reagent, ProLong (Molecular Probes, Eugene, OR, USA), stored in the dark at 4°C, and examined within 1−3 days. Stained slides were examined with a Zeiss Axioplan 2 imaging microscope, and representative images were automatically taken using a digital spot camera. The original magnifications were × 200.

Statistical analysis

Data are mean ± s.d. unless specified. The statistical significance of differences noted in the biochemical parameters was evaluated using one-way analysis of variance. Pearson's correlation coefficient was used to evaluate the associations between renal function tests and blood lipid levels. A *P*-value of less than 0.05 was taken as a criterion for a statistically significant difference.

DISCLOSURE

All the authors declared no competing interests.

ACKNOWLEDGMENTS

This study was partly funded by the Graduate School of the Chinese University of Hong Kong and by a grant from the Research Grants Council of the Hong Kong Special Administrative Region, China (CUHK4462/06M). We gratefully acknowledge the technical assistance of Stanley Ho.

REFERENCES

1. Kida K, Nakajo S, Kamiya F *et al.* Renal net glucose release *in vivo* and its contribution to blood glucose in rats. *J Clin Invest* 1978; **62**: 721–726.
2. McGuinness OP, Fugiwara T, Murrell S *et al.* Impact of chronic stress hormone infusion on hepatic carbohydrate metabolism in the conscious dog. *Am J Physiol* 1993; **265**: E314–E322.
3. Stumvoll M, Chintalapudi U, Perriello G *et al.* Uptake and release of glucose by the human kidney. Postabsorptive rates and responses to epinephrine. *J Clin Invest* 1995; **96**: 2528–2533.
4. Boudville N, Prasad GV, Knoll G *et al.* Meta-analysis: risk for hypertension in living kidney donors. *Ann Intern Med* 2006; **145**: 185–196.
5. Mak RH, DeFronzo RA. Glucose and insulin metabolism in uremia. *Nephron* 1992; **61**: 377–382.
6. Cheung AK, Wu LL, Kablitz C *et al.* Atherogenic lipids and lipoproteins in hemodialysis patients. *Am J Kidney Dis* 1993; **22**: 271–276.
7. Odamaki M, Furuya R, Ohkawa S *et al.* Altered abdominal fat distribution and its association with the serum lipid profile in non-diabetic haemodialysis patients. *Nephrol Dial Transplant* 1999; **14**: 2427–2432.
8. Montani JP, Carroll JF, Dwyer TM *et al.* Ectopic fat storage in heart, blood vessels and kidneys in the pathogenesis of cardiovascular diseases. *Int J Obes Relat Metab Disord* 2004; **28**(Suppl 4): S58–S65.
9. Hull D, Segall MM. Distinction of brown from white adipose tissue. *Nature* 1966; **212**: 469–472.
10. Rothwell NJ, Stock MJ. A role for brown adipose tissue in diet-induced thermogenesis. *Nature* 1979; **281**: 31–35.
11. Avram AS, Avram MM, James WD. Subcutaneous fat in normal and diseased states: 2. Anatomy and physiology of white and brown adipose tissue. *J Am Acad Dermatol* 2005; **53**: 671–683.
12. Zancanaro C, Nano R, Marchioro C *et al.* Magnetic resonance spectroscopy investigations of brown adipose tissue and isolated brown adipocytes. *J Lipid Res* 1994; **35**: 2191–2199.
13. Sekhar BS, Kurup CK, Ramasarma T. Microsomal redox systems in brown adipose tissue: high lipid peroxidation, low cholesterol biosynthesis and no detectable cytochrome P-450. *Mol Cell Biochem* 1990; **92**: 147–157.
14. Arstila AU, Smith MA, Trump BF. Microsomal lipid peroxidation: morphological characterization. *Science* 1972; **175**: 530–533.
15. Harman D. Lipofuscin and ceroid formation: the cellular recycling system. *Adv Exp Med Biol* 1989; **266**: 3–15.
16. Tanuma Y, Tamamoto M, Ito T *et al.* The occurrence of brown adipose tissue in perirenal fat in Japanese. *Arch Histol Jpn* 1975; **38**: 43–70.
17. Santos GC, Araujo MR, Silveira TC *et al.* Accumulation of brown adipose tissue and nutritional status. A prospective study of 366 consecutive autopsies. *Arch Pathol Lab Med* 1992; **116**: 1152–1154.
18. Guebre-Egziabher F, Bernhard J, Funahashi T *et al.* Adiponectin in chronic kidney disease is related more to metabolic disturbances than to decline in renal function. *Nephrol Dial Transplant* 2005; **20**: 129–134.

19. Nagase S, Aoyagi K, Gotoh M *et al.* Increased lipid peroxidation by rat liver microsomes in experimental renal failure. *Nephron* 1996; **74**: 204–208.
20. Van den Branden C, Gabriels M, Vamecq J *et al.* Carvedilol protects against glomerulosclerosis in rat remnant kidney without general changes in antioxidant enzyme status. A comparative study of two beta-blocking drugs, carvedilol and propanolol. *Nephron* 1997; **77**: 319–324.
21. Campbell DJ, Kladis A, Duncan AM. Nephrectomy, converting enzyme inhibition, and angiotensin peptides. *Hypertension* 1993; **22**: 513–522.
22. Cassis LA, Saye J, Peach MJ. Location and regulation of rat angiotensinogen messenger RNA. *Hypertension* 1988; **11**: 591–596.
23. Grond J, van Goor H, Erkelens DW *et al.* Glomerular sclerotic lesions in the rat. Histochemical analysis of their macromolecular and cellular composition. *Virchows Arch B Cell Pathol Incl Mol Pathol* 1986; **51**: 521–534.
24. Williams AJ, Walls J. Body composition changes in the subtotally nephrectomized rat fed differing dietary proteins. *Nephron* 1989; **51**: 384–387.
25. Fujihara CK, Limongi DM, Falzone R *et al.* Pathogenesis of glomerular sclerosis in subtotally nephrectomized analbuminemic rats. *Am J Physiol* 1991; **261**: F256–F264.
26. Rutkowski B, Szolkiewicz M, Korczynska J *et al.* The role of lipogenesis in the development of uremic hyperlipidemia. *Am J Kidney Dis* 2003; **41**: S84–S88.
27. Szolkiewicz M, Nieweglowski T, Korczynska J *et al.* Upregulation of fatty acid synthase gene expression in experimental chronic renal failure. *Metabolism* 2002; **51**: 1605–1610.
28. Bagdade JD, Yee E, Wilson DE *et al.* Hyperlipidemia in renal failure: studies of plasma lipoproteins, hepatic triglyceride production, and tissue lipoprotein lipase in a chronically uremic rat model. *J Lab Clin Med* 1978; **91**: 176–186.
29. Jacobs DB, Hayes GR, Truglia JA *et al.* Alterations of glucose transporter systems in insulin-resistant uremic rats. *Am J Physiol* 1989; **257**: E193–E197.
30. Swierczynski J, Korczynska J, Szolkiewicz M *et al.* Low leptin mRNA level in adipose tissue and normoleptinemia in experimental chronic renal failure. *Exp Nephrol* 2001; **9**: 54–59.
31. Vaziri ND, Wang XQ, Liang K. Secondary hyperparathyroidism downregulates lipoprotein lipase expression in chronic renal failure. *Am J Physiol* 1997; **273**: F925–F930.
32. Vaziri ND, Liang K. Down-regulation of tissue lipoprotein lipase expression in experimental chronic renal failure. *Kidney Int* 1996; **50**: 1928–1935.
33. Vaziri ND, Liang K. Down-regulation of VLDL receptor expression in chronic experimental renal failure. *Kidney Int* 1997; **51**: 913–919.
34. Heuck CC, Liersch M, Ritz E *et al.* Hyperlipoproteinemia in experimental chronic renal insufficiency in the rat. *Kidney Int* 1978; **14**: 142–150.
35. Axelsson J, Stenvinkel P. Role of fat mass and adipokines in chronic kidney disease. *Curr Opin Nephrol Hypertens* 2008; **17**: 25–31.
36. de Vinuesa SG, Goicoechea M, Kanter J *et al.* Insulin resistance, inflammatory biomarkers, and adipokines in patients with chronic kidney disease: effects of angiotensin II blockade. *J Am Soc Nephrol* 2006; **17**: S206–S212.
37. Stenvinkel P, Marchlewska A, Pecoits-Filho R *et al.* Adiponectin in renal disease: relationship to phenotype and genetic variation in the gene encoding adiponectin. *Kidney Int* 2004; **65**: 274–281.
38. Tanuma Y, Ohata M, Ito T *et al.* Possible function of human brown adipose tissue as suggested by observation on perirenal brown fats from necropsy cases of variable age groups. *Arch Histol Jpn* 1976; **39**: 117–145.
39. Rayner HC, Ross-Gilbertson VL, Walls J. The role of lipids in the pathogenesis of glomerulosclerosis in the rat following subtotal nephrectomy. *Eur J Clin Invest* 1990; **20**: 97–104.
40. Rayner HC, Ward L, Walls J. Cholesterol feeding following unilateral nephrectomy in the rat leads to glomerular hypertrophy. *Nephron* 1991; **57**: 453–459.
41. van Goor H, Fidler V, Weening JJ *et al.* Determinants of focal and segmental glomerulosclerosis in the rat after renal ablation. Evidence for involvement of macrophages and lipids. *Lab Invest* 1991; **64**: 754–765.
42. Hahn S, Kuemmerle NB, Chan W *et al.* Glomerulosclerosis in the remnant kidney rat is modulated by dietary alpha-tocopherol. *J Am Soc Nephrol* 1998; **9**: 2089–2095.
43. Van den Branden C, Verelst R, Vamecq J *et al.* Effect of vitamin E on antioxidant enzymes, lipid peroxidation products and glomerulosclerosis in the rat remnant kidney. *Nephron* 1997; **76**: 77–81.
44. Kasiske BL, O'Donnell MP, Garvis WJ *et al.* Pharmacologic treatment of hyperlipidemia reduces glomerular injury in rat 5/6 nephrectomy model of chronic renal failure. *Circ Res* 1988; **62**: 367–374.
45. Glazer AA, Inman SR, Stowe NT *et al.* Renal microcirculatory effects of lovastatin in a rat model of reduced renal mass. *Urology* 1997; **50**: 812–817.
46. Coresh J, Byrd-Holt D, Astor BC *et al.* Chronic kidney disease awareness, prevalence, and trends among U.S. adults, 1999–2000. *J Am Soc Nephrol* 2005; **16**: 180–188.
47. Jolma P, Koobi P, Kalliovalkama J *et al.* Increased calcium intake reduces plasma cholesterol and improves vasorelaxation in experimental renal failure. *Am J Physiol Heart Circ Physiol* 2003; **285**: H1882–H1889.